Dynamic crystallization in a quantum Ising chain

K. L. Zhang and Z. Song [*]
School of Physics, Nankai University, Tianjin 300071, China

(Received 20 April 2020; accepted 27 July 2020; published 13 August 2020)

The topological degeneracy of ground states in transverse field Ising chain cannot be removed by local perturbation and allows it to be a promising candidate for topological computation. We study the dynamic processes of crystallization and dissolution for the gapped ground states in an Ising chain. For this purpose, the real-space renormalization method is employed to build an effective Hamiltonian that captures the low-energy physics of a given system. We show that the ground state and the first-excited state of an $(N+1)$-site chain can be generated from that of the N-site one by adding a spin adiabatically and vice versa. Numerical simulation shows that the robust quasidegenerate ground states of finite-size chain can be prepared with high fidelity from a set of noninteracting spins by a quasiadiabatic process. As an application, we propose a scheme for entanglement transfer between a pair of spins and two separable Ising chains as macroscopic topological qubits.

DOI: 10.1103/PhysRevA.102.022211

I. INTRODUCTION

The transverse field Ising model [1] is a paradigm in both traditional second-order quantum phase transition (QPT) based on spontaneous symmetry breaking [2] and topological QPT, which is immune to local perturbation [3,4]. One of the most remarkable features of the one-dimensional Ising chain is that its topological degenerate ground states are protected from higher-energy excitations by the energy gap, and are characterized by the existence of Majorana edge states, which are robust to perturbations [5]. In the past few decades, the numerical calculations [6–10] and experimental investigation [11–14] in quasi-one-dimensional complex compounds triggered the study of macroscopic quantum phenomena in quantum spin systems [15,16] . It has been reported that an interacting Ising spin chain can be simulated by using Mott insulator spinless bosons in a tilted optical lattice [17]. And the ground states of spin-1 antiferromagnetic Heisenberg chain, which possesses a topological phase of matter known as the Haldane phase [18–20], are also experimentally achievable [21–23]. A promising application of such quantum spin systems is physical implementation of quantum information processing devices based on a solid-state system [24–28]. Thanks to the intrinsic stability of the topological feature, a system with topological phase can be a promising platform for quantum computation and information processing [29–31]. It motivates us to develop an alternative candidate for a macroscopic qubit based on the Ising chain in the topological phase, due to the fact that its degenerate ground states are robust against the disordered perturbation.

In this work, we explore a way to prepare the ground state and the first-excited state of an Ising chain on demand by dynamic process of crystallization, generating robust macroscopic quantum states against disordered perturbation. Based on an analytical perturbation analysis, we employ a real-space renormalization method to build an effective Hamiltonian that captures the low-energy physics of a given system. Within the topological nontrivial region, the effective Hamiltonian for an $(N+1)$-site chain is obtained from the ground state and first-excited state of an N-site chain. It is a modified two-spin Ising model, which is exactly solvable and allows one to design an adiabatic passage for crystallization or dissolution. We show that the ground state and the first-excited state of an $(N+1)$-site chain can be generated from that of the N-site one by adding a spin adiabatically and vice versa. Starting from $N=1$, as a seed crystal, numerical simulation is performed for the quasiadiabatic process, confirming our prediction. As an application in quantum information processing, we demonstrate the scheme of entanglement transfer between a pair of qubits and two Ising chains, as macroscopic objects.

This paper is organized as follows. In Sec. II, we present the model and its symmetries. In Sec. III, an effective Hamiltonian that captures the low-energy physics is obtained based on a real-space renormalization method. In Sec. IV, we propose an adiabatic passage for crystallization, which generates the ground state and the first-excited state of a finite-size chain from simple spin configurations. It allows the scheme of entanglement transfer from two qubits to two Ising chains, creating a macroscopic entangled state. In Sec. V, we investigate the robustness of the ground states in the presence of quenched disordered perturbation. We also propose an adiabatic passage for entanglement distillation from an obtained macroscopic entangled state. Section VI summarizes the results and explores their implications.

II. MODEL AND SYMMETRIES

We consider the Hamiltonian of a transverse field Ising model

$$H=\sum_{j=1}^{N-1} J_j \sigma_j^x \sigma_{j+1}^x+\sum_{j=1}^{N} g_j \sigma_j^z, \tag{1}$$

[*]songtc@nankai.edu.cn

on a chain with open boundary condition, where σ_j^α ($\alpha = x,\ y,\ z$) are the Pauli operators on site j and parameters J_j and g_j are position and time dependent, without losing the generality. The second term and quantity $\sigma^z = \sum_{j=1}^{N} \sigma_j^z$ have common eigenstates, and the first term breaks the conservation of this quantity. However, the parity of the eigenvalue of σ^z is conservative, i.e., we always have

$$[p, H] = 0, \tag{2}$$

where the parity operator

$$p = \prod_{j=1}^{N} \left(-\sigma_j^z\right). \tag{3}$$

We start from the simple case with uniform parameters, $J_j = J$ and $g_j = g$, to analyze the property of the ground state. For finite N, the parity of ground state with nonzero g can be determined by the ground state in the $g = \pm\infty$ limit. It is due to the fact of nondegeneracy of the ground state for finite N and nonzero g. Actually, it has been shown that the spectrum of H can be constructed based on the positive levels of the corresponding Su-Schrieffer-Heeger (SSH) chain [5,32]. The nonzero energy levels of an SSH chain result in the fact that the ground-state energy is nondegenerate except at $g = 0$. Here we give the conclusions of the parity of ground state: (i) for even N, we have $p = 1$ for the ground state with any $g \neq 0$, while (ii) for odd N, we have $p = \mathrm{sgn}(g)$.

For a finite N system with a periodic boundary condition, the exact solution can be obtained [1] and the ground state obeys the same rule. It is the common sense that the property of the model is not sensitive to the boundary condition in the thermodynamic limit. Nevertheless, here we would like to emphasize that the Hamiltonian with infinite N possesses an exclusive symmetry in the topological nontrivial region $0 < |g/J| < 1$. It can be checked that there exists a nonlocal spin operator (see the Appendix)

$$D_N = \frac{1}{2}\sqrt{1 - \left(\frac{g}{J}\right)^2} \sum_{j=1}^{N} \prod_{l<j} \left(-\sigma_l^z\right) \times \left[\left(-\frac{g}{J}\right)^{j-1} \sigma_j^x - i\left(-\frac{g}{J}\right)^{N-j} \sigma_j^y\right], \tag{4}$$

satisfying the commutation relations

$$[D_N, H] = [D_N^\dagger, H] = 0, \tag{5}$$

$$\{D_N, D_N^\dagger\} = 1, \quad (D_N)^2 = (D_N^\dagger)^2 = 0, \tag{6}$$

Besides the method presented in the Appendix, D_N can also be obtained by using the iterative method presented in Ref. [33], in which Ψ is a Majorana operator, while D_N is a fermion operator satisfying Eq. (6). The term $\prod_{l<j}(-\sigma_l^z)$ in D_N is similar to the ν_l operators in Ref. [34], and they both arise from the transformation between spin operators and fermion operators. We would like to point out that the commutation relation in Eq. (5) can be regarded as a symmetry of the system. Importantly, such a symmetry is conditional, requiring $0 < |g/J| < 1$, large N limit, and open boundary condition. The first two conditions are in accord with the symmetry breaking mechanism for QPT [2]. The transverse field Ising model with periodic boundary condition [1] breaks the symmetry Eq. (5). This can be related to the fact that the SSH chain supports two zero-eigenenergy edge states in the topological nontrivial region (see the Appendix), while the SSH ring does not support these two modes.

Furthermore, the commutation relation in Eq. (5) guarantees the existence of degeneracy of the eigenstates. There might be a set of degenerate eigenstates $\{|\psi_n^+\rangle, |\psi_n^-\rangle\}$ of H with eigenenergy E_n, in two invariant subspaces, i.e.,

$$H|\psi_n^\pm\rangle = E_n|\psi_n^\pm\rangle \tag{7}$$

and

$$p|\psi_n^\pm\rangle = \pm|\psi_n^\pm\rangle. \tag{8}$$

Importantly, we have the relations

$$D_N|\psi_n^+\rangle = |\psi_n^-\rangle, \quad D_N^\dagger|\psi_n^-\rangle = |\psi_n^+\rangle,$$
$$D_N^\dagger|\psi_n^+\rangle = D_N|\psi_n^-\rangle = 0. \tag{9}$$

Especially, applying the operator D_N ($D_N^\dagger$) on the lowest-energy eigenstates $|\psi_{\mathrm{g}}^+\rangle$ and $|\psi_{\mathrm{g}}^-\rangle$ of H in two invariant subspaces, we have

$$D_N|\psi_{\mathrm{g}}^+\rangle = |\psi_{\mathrm{g}}^-\rangle, \quad D_N^\dagger|\psi_{\mathrm{g}}^-\rangle = |\psi_{\mathrm{g}}^+\rangle,$$
$$D_N^\dagger|\psi_{\mathrm{g}}^+\rangle = D_N|\psi_{\mathrm{g}}^-\rangle = 0, \tag{10}$$

and then $|\psi_{\mathrm{g}}^+\rangle$ and $|\psi_{\mathrm{g}}^-\rangle$ are degenerate ground states. In the rest of this paper, we denote eigenstates $|\psi_{\mathrm{g}}^+\rangle$ and $|\psi_{\mathrm{g}}^-\rangle$ by $|\psi_{\mathrm{g}}^N\rangle$ and $|\psi_{\mathrm{e}}^N\rangle$, representing the ground state and the first-excited state, respectively.

Such a symmetry is also responsible for the topological degeneracy. In fact, there also exists an operator D_N for the Hamiltonian in the presence of slight disordered deviations on the uniform $J_j = J$ and $g_j = g$, since the edge modes of the SSH chain are robust against disordered perturbation (see the Appendix). Thus the degeneracy of ground states cannot be lifted by local perturbation. It is desirable to employ such two states as two orthonormal basis states of a topological qubit. To this end, a basic task is to find a way to prepare the ground state and the first-excited state (which are quasidegenerate) of the Ising chain.

III. EFFECTIVE HAMILTONIAN

In this section, we aim to establish the connection between a single spin and an Ising chain. We will provide a way to generate the ground state and the first-excited state of an $(N+1)$-site Ising chain from that of the N -site one. To proceed, we consider a system which consists of two parts, an Ising chain and a single spin. The Hamiltonian has the form

$$H^{(N+1)} = H_0 + H', \tag{11}$$

$$H_0 = J\sum_{i=1}^{N-1} \sigma_i^x\sigma_{i+1}^x + g\sum_{i=1}^{N} \sigma_i^z + g\sigma_{N+1}^z, \tag{12}$$

with $0 < g \ll J$, and the coupling between them is Ising type

$$H' = \lambda\sigma_N^x\sigma_{N+1}^x, \tag{13}$$

with positive parameter $\lambda \ll J$. Here the N-site Ising chain $H_0 - g\sigma_{N+1}^z$ has gapped low-lying eigenstates $|\psi_{\mathrm{e}}^N\rangle$ and $|\psi_{\mathrm{g}}^N\rangle$

with energy $E_{\mathrm{e}}^{(N)}$ and $E_{\mathrm{g}}^{(N)}$, respectively, and the gap is sufficiently large, so that $H' = \lambda(\sigma_N^+ + \sigma_N^-)(\sigma_{N+1}^+ + \sigma_{N+1}^-)$ can be regarded as perturbation. By adiabatically eliminating the excited levels, we obtain an effective Hamiltonian

$$H_{\mathrm{eff}}^{(N+1)} = J_{\mathrm{eff}}^{(N)}\sigma_0^x\sigma_{N+1}^x + g_{\mathrm{eff}}^{(N)}\sigma_0^z + g\sigma_{N+1}^z + \frac{E_{\mathrm{e}}^{(N)} + E_{\mathrm{g}}^{(N)}}{2}, \tag{14}$$

where the Pauli matrices σ_0^x and σ_0^z are defined as

$$\begin{aligned}\sigma_0^x|\psi_{\mathrm{e}}^N\rangle &= |\psi_{\mathrm{g}}^N\rangle, \quad \sigma_0^x|\psi_{\mathrm{g}}^N\rangle = |\psi_{\mathrm{e}}^N\rangle,\\ \sigma_0^z|\psi_{\mathrm{e}}^N\rangle &= |\psi_{\mathrm{e}}^N\rangle, \quad \sigma_0^z|\psi_{\mathrm{g}}^N\rangle = -|\psi_{\mathrm{g}}^N\rangle.\end{aligned} \tag{15}$$

And the effective coupling and field are

$$\begin{aligned}J_{\mathrm{eff}}^{(N)} &= \lambda\langle\psi_{\mathrm{g}}^N|(\sigma_N^+ + \sigma_N^-)|\psi_{\mathrm{e}}^N\rangle,\\ g_{\mathrm{eff}}^{(N)} &= \frac{E_{\mathrm{e}}^{(N)} - E_{\mathrm{g}}^{(N)}}{2}.\end{aligned} \tag{16}$$

The effective Hamiltonian $H_{\mathrm{eff}}^{(N+1)}$ is a modified two-site Ising model if $g_{\mathrm{eff}}^{(N)} \neq g$, describing low-lying eigenstates of the original Hamiltonian $H^{(N+1)}$ in Eq. (11).

We readily obtain the ground state and the first-excited state of the effective Hamiltonian $H_{\mathrm{eff}}^{(N+1)}$, which are

$$|\psi_{\mathrm{eff}}^{\mathrm{g}}\rangle = \frac{1}{\sqrt{1+(\xi_N^+)^2}}\left(|\psi_{\mathrm{g}}^N\rangle|\downarrow\rangle_{N+1} - \xi_N^+|\psi_{\mathrm{e}}^N\rangle|\uparrow\rangle_{N+1}\right) \tag{17}$$

and

$$|\psi_{\mathrm{eff}}^{\mathrm{e}}\rangle = \frac{1}{\sqrt{1+(\xi_N^-)^2}}\left(|\psi_{\mathrm{e}}^N\rangle|\downarrow\rangle_{N+1} - \xi_N^-|\psi_{\mathrm{g}}^N\rangle|\uparrow\rangle_{N+1}\right), \tag{18}$$

with energies

$$E_{\mathrm{eff}}^{\mathrm{g}} = \frac{E_{\mathrm{e}}^{(N)} + E_{\mathrm{g}}^{(N)}}{2} - \Lambda_N^+ \tag{19}$$

and

$$E_{\mathrm{eff}}^{\mathrm{e}} = \frac{E_{\mathrm{e}}^{(N)} + E_{\mathrm{g}}^{(N)}}{2} - \Lambda_N^-, \tag{20}$$

respectively, where the coefficients

$$\begin{aligned}\xi_N^\pm &= \frac{J_{\mathrm{eff}}^{(N)}}{g \pm g_{\mathrm{eff}}^{(N)} + \Lambda_N^\pm},\\ \Lambda_N^\pm &= \sqrt{\left[g \pm g_{\mathrm{eff}}^{(N)}\right]^2 + \left[J_{\mathrm{eff}}^{(N)}\right]^2}.\end{aligned} \tag{21}$$

We note that, in the case of

$$g \pm g_{\mathrm{eff}}^{(N)} > 0, \tag{22}$$

the ground state and the first-excited state reduce to $|\psi_{\mathrm{g}}^N\rangle|\downarrow\rangle_{N+1}$ and $|\psi_{\mathrm{e}}^N\rangle|\downarrow\rangle_{N+1}$, respectively, when $J_{\mathrm{eff}}^{(N)} = 0$. This is crucial for the present work. A straightforward conclusion is that the ground state and the first-excited state $|\psi_{\mathrm{g}}^{N+1}\rangle$ and $|\psi_{\mathrm{e}}^{N+1}\rangle$ of an $(N+1)$-site chain can be obtained by adding a down spin $|\downarrow\rangle_{N+1}$, and then adiabatically increasing λ from 0 to J. The explicit expressions are

$$\mathcal{U}(H')|\psi_{\mathrm{g}}^N\rangle|\downarrow\rangle_{N+1} = |\psi_{\mathrm{g}}^{N+1}\rangle, \tag{23}$$

$$\mathcal{U}(H')|\psi_{\mathrm{e}}^N\rangle|\downarrow\rangle_{N+1} = |\psi_{\mathrm{e}}^{N+1}\rangle, \tag{24}$$

where

$$\mathcal{U}(H') = \mathcal{T}\exp\left[-i\int_0^\infty H'(t)dt\right] \tag{25}$$

is the propagator of the Hamiltonian $H'(t) = \lambda(t)\sigma_N^x\sigma_{N+1}^x$, with $\lambda(t)$ being a very slow function as an adiabatic passage, fulfilling $\lambda(0) = 0$ and $\lambda(\infty) = J$. Here, $\mathcal{T}$ is the time-ordering operator. The valid maximum value of $d\lambda(t)/dt$ depends on the energy gap between two low-lying states and the higher excited states. Then, due to the protection of the energy gap, the higher excitations are not affected.

IV. DYNAMIC CRYSTALLIZATION

So far, we have shown how to map the ground state and the first-excited state of an N-site Ising chain to that of the $(N+1)$-site system. It may provide a way to generate the ground state and the first-excited state of finite-size chain from simple spin configurations by the process of dynamic crystallization. Here, we refer to this process as "crystallization" due to the following reasons: (i) the process is about the noninteracting particles evolving to the coupled array and (ii) the final state is determined by the initial state of the first site as a seed crystal. The schematic illustration of this process is shown in Figs. 1(a) and 1(b) for a five-site system.

We describe such a process by a time-dependent Hamiltonian

$$H_{\mathrm{DC}}(t) = \sum_{i=1}^{N-1} J_i(t)\sigma_i^x\sigma_{i+1}^x + \sum_{i=1}^{N} g_i\sigma_i^z, \tag{26}$$

where $\{J_n(t)\}$ is a series of slow functions fulfilling $J_n(0) = 0$ and $J_n(\infty) = \mathrm{const}$ to switch the couplings along the chain one by one consecutively and quasiadiabatically. A typical form of $\{J_n(t)\}$ is the error function

$$J_n(t) = \frac{\lambda_n}{2}\{\mathrm{erf}[\omega(t - n\tau)] + 1\}, \tag{27}$$

where λ_n is the strength of the final coupling. The shape of function $J_n(t)$ is plotted in Fig. 1(c). In the following, we estimate the possible result, based on the renormalization method. The basic idea is as follows. According to the analysis in the previous section, in the adiabatic regime, the dynamics in the duration of switching on J_i is governed approximately by the effective Hamiltonian in the form

$$H_{\mathrm{eff}}^{(i+1)} = J_{\mathrm{eff}}^{(i)}\sigma_0^x\sigma_{i+1}^x + g_{\mathrm{eff}}^{(i)}\sigma_0^z + g_{i+1}\sigma_{i+1}^z + \frac{E_{\mathrm{eff}}^{\mathrm{e}(i)} + E_{\mathrm{eff}}^{\mathrm{g}(i)}}{2}, \tag{28}$$

where Pauli operators σ_0^x and σ_0^z take actions on the ground state and the first-excited state of the i-site chain; parameters $J_{\mathrm{eff}}^{(i)}$, $g_{\mathrm{eff}}^{(i)}$, $E_{\mathrm{eff}}^{\mathrm{e}(i)}$, and $E_{\mathrm{eff}}^{\mathrm{g}(i)}$ are obtained from $H_{\mathrm{eff}}^{(i)}$. Then $H_{\mathrm{eff}}^{(i+1)}$ generates the parameters in the effective Hamiltonian $H_{\mathrm{eff}}^{(i+2)}$:

$$\begin{aligned}g_{\mathrm{eff}}^{(i+1)} &= \frac{E_{\mathrm{eff}}^{\mathrm{e}(i+1)} - E_{\mathrm{eff}}^{\mathrm{g}(i+1)}}{2}\\ &= \frac{1}{2}(\Lambda_i^+ - \Lambda_i^-)\end{aligned} \tag{29}$$

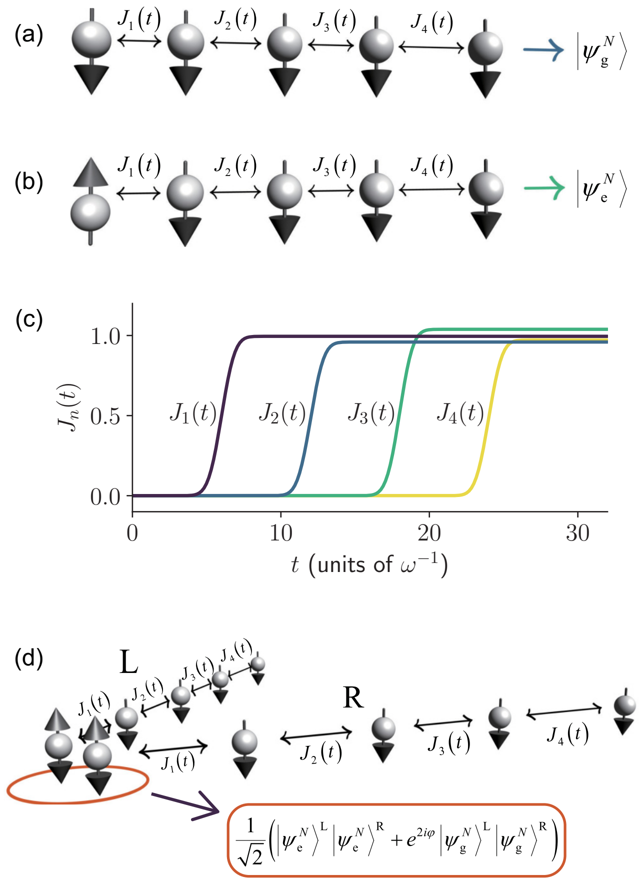

FIG. 1. Panels (a) and (b) are the schematic illustrations of the dynamic crystallization process. The spin configurations in panels (a) and (b) are adiabatically evolving into the ground state and the first-excited state, respectively, by turning on the couplings $\{J_n(t)\}$ one by one adiabatically. (c) Plot of the couplings in the form of Eq. (27) as functions of time t. Here we take $\omega = 0.001$, $\tau = 6$, and $\lambda_n \approx 1$ as an example. (d) Schematic illustration of the entanglement transfer process between a pair of spins and two separable Ising chains.

and

$$J_{\text{eff}}^{(i+1)} = \lambda_i \langle \psi_{\text{eff}}^{g(i+1)} | (\sigma_{i+1}^+ + \sigma_{i+1}^-) | \psi_{\text{eff}}^{e(i+1)} \rangle = -\frac{\lambda_i(\xi_i^+ + \xi_i^-)}{\sqrt{1+(\xi_i^+)^2}\sqrt{1+(\xi_i^-)^2}}. \tag{30}$$

We start from $i = 1$ with $J_{\text{eff}}^{(1)} = \lambda_1$, $g_{\text{eff}}^{(1)} = g_1$, and $E_{\text{eff}}^{e(1)} = -E_{\text{eff}}^{g(1)} = g_1$, i.e.,

$$H_{\text{eff}}^{(2)} = \lambda_1 \sigma_1^x \sigma_2^x + g_1 \sigma_1^z + g_2 \sigma_2^z, \tag{31}$$

which is a two-site Ising model. Then effective parameters $g_{\text{eff}}^{(i)}$ and $J_{\text{eff}}^{(i)}$ with $i > 1$ are obtained by the iteration from Eqs. (29) and (30) or $H_{\text{eff}}^{(i)}$. In order to verify the proposed approximate approach, we compare the strength of effective field $g_{\text{eff}}^{(i)}$ obtained from the renormalization method in Eq. (29) and the exact diagonalization method. The plots in Fig. 2 show that for small g and large i (N), the approximate results have relatively small errors.

Importantly, when a set of obtained parameters $\{g_{\text{eff}}^{(i)}\}$ satisfies the condition

$$g_{i+1} \pm g_{\text{eff}}^{(i)} > 0, \tag{32}$$

we have

$$\mathcal{U}(H_{\text{DC}})(\alpha|\uparrow\rangle_1 + \beta|\downarrow\rangle_1)\prod_{l=2}^{N}|\downarrow\rangle_l = \alpha|\psi_e^N\rangle + e^{i\varphi}\beta|\psi_g^N\rangle, \tag{33}$$

where $\mathcal{U}(H_{\text{DC}}) = \mathcal{T}\exp[-i\int_0^\infty H_{\text{DC}}(t)dt]$ and φ is a dynamical phase. This process is similar to that of dynamic crystallization in the case $\alpha = 0$ or $\beta = 0$. Here the first spin at state $|\uparrow\rangle_1(|\downarrow\rangle_1)$ takes the role of a seed crystal, which determines the state $|\psi_e^N\rangle(|\psi_g^N\rangle)$ of the crystal with large N. We demonstrate the dynamic crystallization by numerical simulation in a finite-size system. We use the overlap $O(t) = |\langle\Psi_T|\Psi(t)\rangle|$ between the target state $|\Psi_T\rangle = |\psi_g^N\rangle(|\psi_e^N\rangle)$ obtained from numerical diagonalization and the evolved state

$$|\Psi(t)\rangle = \mathcal{T}\exp\left[-i\int_0^t H_{\text{DC}}(t')dt'\right]|\Psi(0)\rangle, \tag{34}$$

where $|\Psi(0)\rangle = |\downarrow\rangle_1(|\uparrow\rangle_1)\prod_{l=2}^{N}|\downarrow\rangle_l$, to measure the efficiency of the process. The overlaps $O(t)$ are plotted in Fig. 3(a). Meanwhile, as a time reversal of the crystallization process, the simulation for the dissolution process is also performed [see Fig. 3(b)], where the corresponding initial state and target state are $|\Psi(0)\rangle = |\psi_g^N\rangle(|\psi_e^N\rangle)$ and $|\Psi_T\rangle = |\downarrow\rangle_1(|\uparrow\rangle_1)\prod_{l=2}^{N}|\downarrow\rangle_l$. Here the computation is performed by using a uniform mesh in the time discretization for the time-dependent Hamiltonian $H_{\text{DC}}(t)$. The results are in accord with our predictions for both processes.

We would like to point out that the dynamic crystallization process cannot map a qubit state onto a many-qubit two-level state due to the uncertainty of the phase φ. However, as an application in quantum information processing, this makes it possible to realize the entanglement transfer from a pair of qubits to two independent Ising chains, as macroscopic objects. Entanglement is considered to be one of the most profound features of quantum mechanics [35,36] and a very powerful resource for quantum information processing and communication. Specifically, robust and long-lived entanglement of material objects is a desirable task in quantum information processing, including teleportation of quantum states of matter and quantum memory [37]. Here we propose a scheme to generate robust entanglement between two quantum spin chains, as macroscopic objects.

The system we are concerned with is a simple extension of the original system, described by the Hamiltonian

$$H_{\text{D}} = H^{\text{L}} + H^{\text{R}}, \tag{35}$$

where H^{L} and H^{R} represent two independent but identical Ising chains described by Eq. (1), respectively. Consider an initial state, in which the first two spins are maximally entangled, being state $(|\uparrow\rangle_1^{\text{L}}|\uparrow\rangle_1^{\text{R}} + |\downarrow\rangle_1^{\text{L}}|\downarrow\rangle_1^{\text{R}})/\sqrt{2}$. Applying the

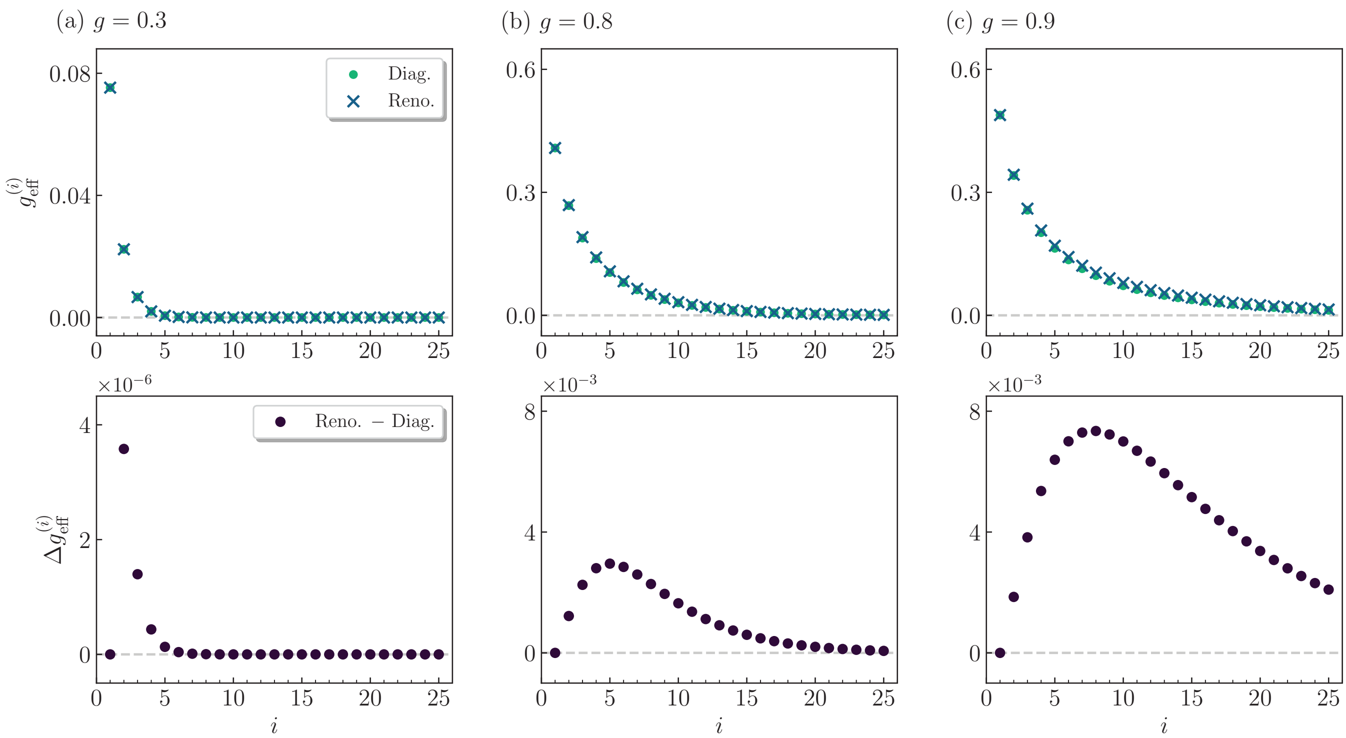

FIG. 2. Comparison between the strength of effective field $g_{\rm eff}^{(i)}$ in Eq. (29) obtained from the renormalization method and the exact diagonalization method. The upper panel is the results obtained from the two methods and the lower panel shows the difference between them. The parameters are $g_i = g = 0.3$, 0.8, and 0.9 ($i \neq 1$) for panels (a), (b), and (c), respectively. Other parameters are $J_i = \lambda = 1$ and $g_1 = 0.9g$. We can see that, for the case of $g \ll 1$ and large i (N), the results obtained from the renormalization method have relatively small errors.

process in Eq. (33), we have

$$\frac{1}{\sqrt{2}}\mathcal{U}(H_{\rm D})\left(|\uparrow\rangle_1^{\rm L}|\uparrow\rangle_1^{\rm R} + |\downarrow\rangle_1^{\rm L}|\downarrow\rangle_1^{\rm R}\right)\prod_{l=2}^{N}|\downarrow\rangle_l^{\rm L}\prod_{l=2}^{N}|\downarrow\rangle_l^{\rm R}$$
$$= \frac{1}{\sqrt{2}}\left(\left|\psi_{\rm e}^{N}\right\rangle^{\rm L}\left|\psi_{\rm e}^{N}\right\rangle^{\rm R} + e^{i2\varphi}\left|\psi_{\rm g}^{N}\right\rangle^{\rm L}\left|\psi_{\rm g}^{N}\right\rangle^{\rm R}\right). \tag{36}$$

This represents entanglement transfer from two spins to two independent Ising chains, keeping the maximal concurrence no matter what the value of φ. Such a process is schematically illustrated in Fig. 1(d).

V. QUENCHED DISORDERED PERTURBATION AND ENTANGLEMENT DISTILLATION

In this section, we focus on the many-particle qubit in two aspects. (i) We demonstrate the robustness of the macroscopic qubit state in the presence of quenched disordered perturbation via a numerical simulation in finite systems. (ii) We propose a scheme to distill the entanglement of two Ising chains via a dissolution process, which transfers the entanglement from chains to a fixed pair of spins.

A. Quenched disordered perturbation

The advantage of the proposed many-particle qubit is that the quasidegenerate ground states of an Ising chain are robust against local perturbation. Technically speaking, there always exists a D_N operator even when parameters J_j and g_j are slightly random (see the Appendix). This means that the degeneracy cannot be lifted when the random perturbation is induced adiabatically. Then, during the process, $\alpha|\psi_{\rm e}^N(0)\rangle + \beta|\psi_{\rm g}^N(0)\rangle$ evolves to $\alpha|\psi_{\rm e}^N(t)\rangle + \beta|\psi_{\rm g}^N(t)\rangle$, without an extra time-dependent phase difference on α and β, keeping the original quantum information. Here $|\psi_{\rm g}^N(t)\rangle$ and $|\psi_{\rm e}^N(t)\rangle$ are instantaneous ground state and first-excited state of the time-dependent Hamiltonian. However, in practice, the appearance of disordered perturbation from the environment is random in time. In the following we consider an extreme case, in which a disordered perturbation is added as a quenching process, and investigate the effect of quenched disordered perturbation on a many-spin qubit initial state $|\Psi(0)\rangle = \alpha|\psi_{\rm e}^N(0)\rangle + \beta|\psi_{\rm g}^N(0)\rangle$ by employing numerical simulation for the time evolution on a finite N system. We add a time-dependent perturbation $H_{\rm Ran}$ to the uniform N-site Ising chain. Here $H_{\rm Ran}$ takes the form

$$H_{\rm Ran} = \sum_{j=1}^{N-1}\Delta J_j\sigma_j^x\sigma_{j+1}^x + \sum_{j=1}^{N}\Delta g_j\sigma_j^z, \tag{37}$$

in which the parameters take the Heaviside function of time. We consider the following two cases. (i) The coupling is homogeneous and the field is random:

$$\begin{aligned}\Delta J_j &= 0,\\ \Delta g_j &= \tfrac{1}{2}g_0\Delta_j^g[\mathrm{sgn}(t)+1].\end{aligned} \tag{38}$$

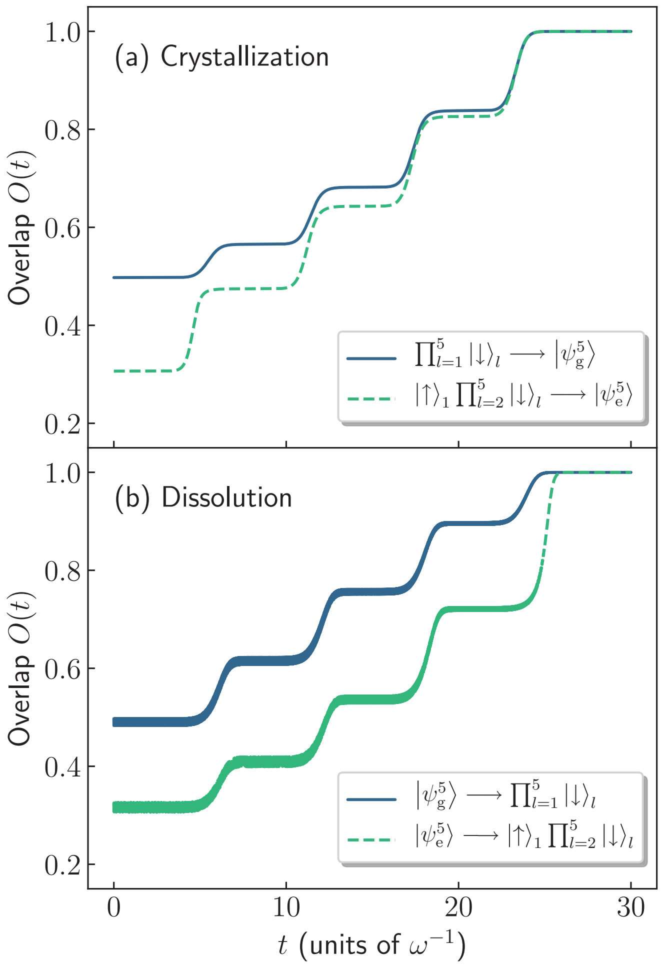

FIG. 3. Numerical results of the overlaps between target states and evolved states for a five-site Ising chain. In the legends, the initial (target) states are on the left (right) side of the arrows. (a) The dynamic crystallization process. The ground (first-excited) state is generated through numerical diagonalization for a uniform Ising chain with parameters $J = 1$, $g = 0.4$, and $N = 5$. The time-dependent Hamiltonian is taken as the form in Eq. (26) with the couplings $\{J_n(t)\}$ in the form of Eq. (27). The parameters are $g_i = g$ $(i \neq 1)$, $g_1 = 0.9g$, $\omega = 0.001$, $\tau = 6$, and $\lambda_n = 1$. (b) The dynamic dissolution process, which can be regarded as a time reversal of the crystallization process. In contrast to the crystallization process, here the initial state is taken as the ground (first-excited) state of the Ising chain, and the couplings $\{J_n(t)\}$ are removed one by one adiabatically.

(ii) Both the coupling and the field are random:

$$\Delta J_j = \tfrac{1}{2}J_0\Delta_j^J[\mathrm{sgn}(t)+1],$$
$$\Delta g_j = \tfrac{1}{2}g_0\Delta_j^g[\mathrm{sgn}(t)+1]. \tag{39}$$

Here $\{\Delta_j^g, \Delta_j^J\}$ denotes a set of uniformly distributed random numbers within the interval $(-R, R)$, taking the role of the disorder strength. We still use the overlap $O(t) = |\langle\Psi(0)|\Psi(t)\rangle|$ between $|\Psi(0)\rangle$ and the evolved state

$$|\Psi(t)\rangle = \exp\left[-i(H + H_{\rm Ran})t\right]|\Psi(0)\rangle \tag{40}$$

to measure the influence of the quenched perturbation. The overlap $O(t)$ for systems with different size and parameters are plotted in Fig. 4. The result with a fixed random strength R shows that, for a fixed N, larger g_0 leads to smaller fidelity, while for a fixed g_0, larger N leads to larger fidelity. This indicates that, even for a finite-size system with $N = 10$, the ground state and the first-excited state are very robust for the case with not large $g_0 < 0.5$.

B. Entanglement distillation

In the following, we turn to demonstrate an adiabatic passage for entanglement distillation from an obtained macroscopic entangled state. To this end, we employ numerical simulation for the time evolution on finite N-site system H in Eq. (1). We start from an initial state $|\Psi(0)\rangle = \alpha|\psi_{\rm e}^N(0)\rangle + \beta|\psi_{\rm g}^N(0)\rangle$. At first step, an arbitrary target spin at site l is selected by decreasing the local field g_l to zero, adiabatically. At second step, after g_l vanishing, we remove the coupling J_j one by one, adiabatically. The order of the dissolution is $J_1 \to 0, J_2 \to 0, \ldots, J_{l-1} \to 0$, and then $J_{N-1} \to 0, J_{N-2} \to 0, \ldots, J_l \to 0$. The above parameters as functions of time are plotted in Figs. 5(a) and 5(b) for a five-site system. During this process, we monitor the evolved state of the spin at site l, by its 2×2 reduced density matrix

$$\rho_l(t) = \mathrm{Tr}_{(l)}[|\Psi(t)\rangle\langle\Psi(t)|], \tag{41}$$

where $\mathrm{Tr}_{(l)}[\ldots]$ denotes taking the trace over all the rest of the freedom. For the initial state $|\Psi(0)\rangle$, the target qubit state is $\alpha|\uparrow\rangle_l + e^{i\varphi}\beta|\downarrow\rangle_l$, which is equivalent to the density matrix $\overline{\rho}_l = \alpha\alpha^*|\uparrow\rangle_l\langle\uparrow|_l + \beta\beta^*|\downarrow\rangle_l\langle\downarrow|_l + e^{-i\varphi}\alpha\beta^*|\uparrow\rangle_l\langle\downarrow|_l + e^{i\varphi}\beta\alpha^*|\downarrow\rangle_l\langle\uparrow|_l$. To describe the efficiency, we employ the trace distance

$$T_l(t) = \tfrac{1}{2}\mathrm{Tr}[\sqrt{[\overline{\rho}_l - \rho_l(t)]^2}], \tag{42}$$

which is a measure of the distinguishability between the evolved state and the target state. We note that the final state $\rho_l(t)$ depends on the adiabatic passage due to the extra dynamic phase φ. Therefore, even though state $\rho_l(t)$ does not meet $\overline{\rho}_l$, it can still be a pure state. We have known that this fact makes it possible for entanglement transfer as mentioned in Eq. (33). Then it is important to measure the purity of the reduced density matrix $\rho_l(t)$, which is defined as

$$\gamma_l(t) = \mathrm{Tr}[\rho_l(t)^2]. \tag{43}$$

The numerical results plotted in Figs. 5(c) and 5(d) show the trace distance $T_l(t)$ and purity $\gamma_l(t)$ as functions of time, verifying our prediction, i.e.,

$$\mathcal{U}(H)\left(\alpha\left|\psi_{\rm e}^N\right\rangle + \beta\left|\psi_{\rm g}^N\right\rangle\right) = (\alpha|\uparrow\rangle_l + e^{i\varphi}\beta|\downarrow\rangle_l)\prod_{j\neq l}^{N}|\downarrow\rangle_j, \tag{44}$$

which is crucial to the scheme of entanglement distillation in the following.

Now we extend the result in Eq. (44) to the two-chain system $H_{\rm D} = H^{\rm L} + H^{\rm R}$. We focus on the entanglement distillation of the two-spin system from two entangled Ising chains. For simplicity, we consider the case with $\alpha = \beta = 1/\sqrt{2}$.

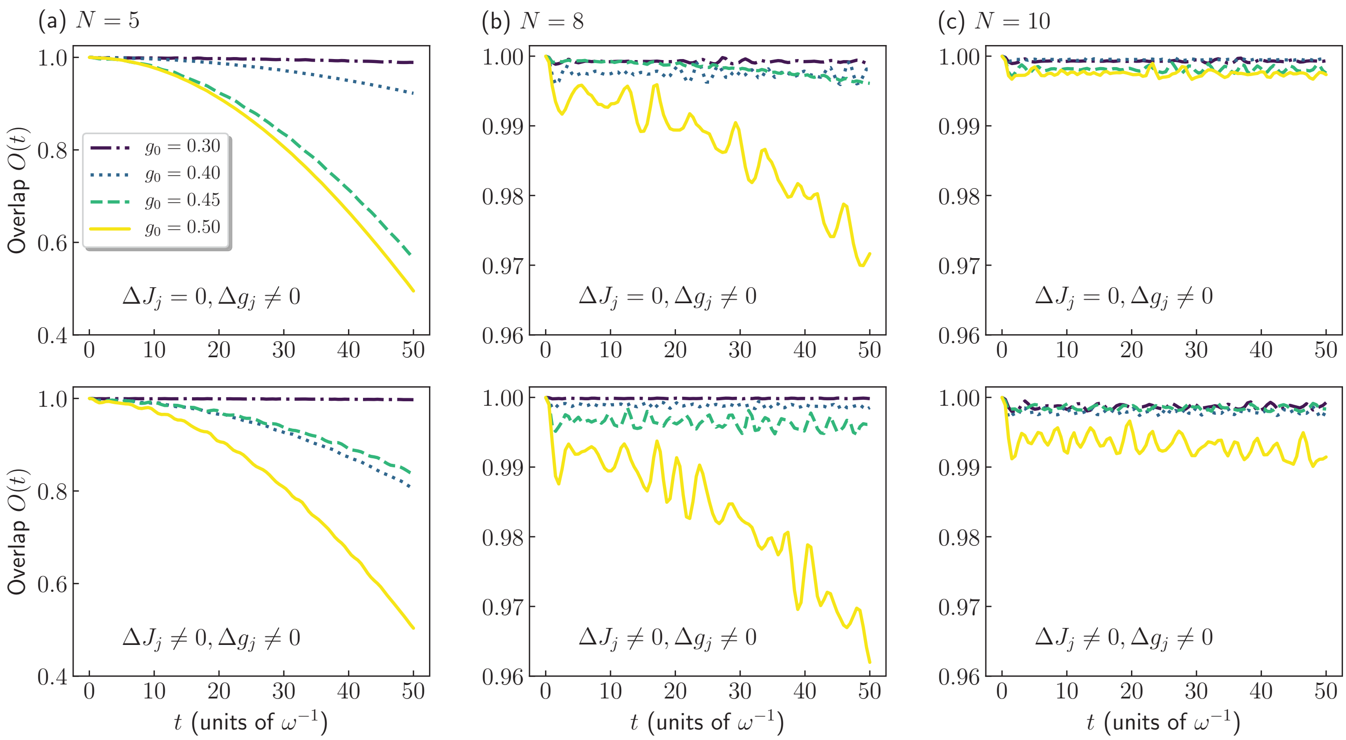

FIG. 4. Numerical results of the overlap between the initial state $|\Psi(0)\rangle$ and its evolved state $|\Psi(t)\rangle$ under two kinds of quenched disordered perturbation in the forms of Eqs. (38) and (39) for different N and g_0. The sizes of the chains are $N = 5$, $N = 8$, and $N = 10$ for panels (a), (b), and (c), respectively. The disorder strength is $R = 0.2$ and the parameters of the uniform Hamiltonian H are $J_j = J_0 = 1$ and $g_j = g_0$. Other parameters are $\alpha = \beta = 1/\sqrt{2}$ and $\omega = 1$.

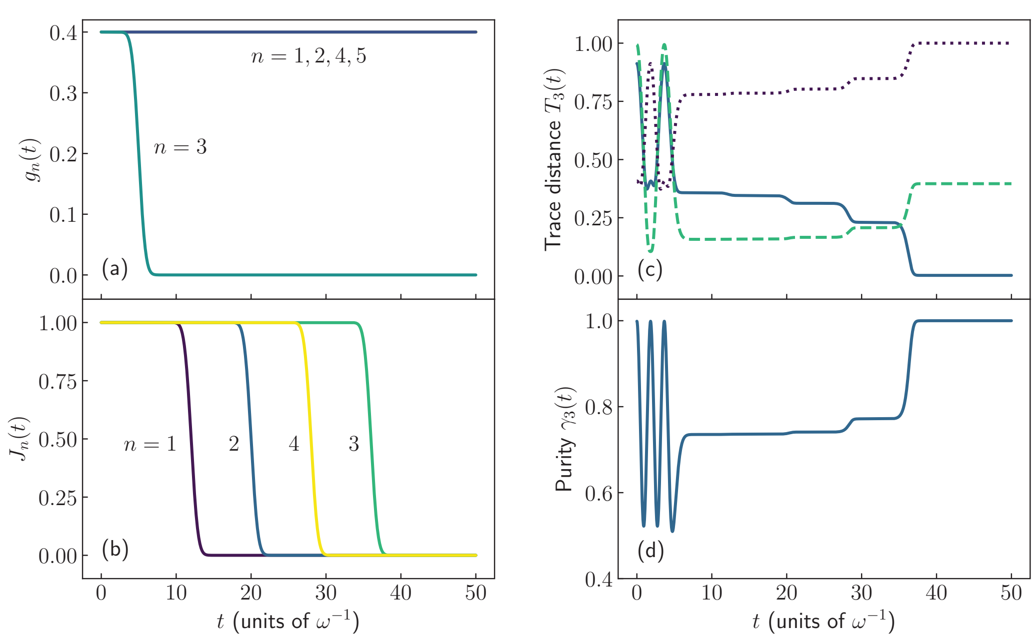

FIG. 5. (a) Adiabatic change of the strength of field $g_n(t)$. The target spin at site $l = 3$ is selected by deceasing the local field g_3 to 0 adiabatically. (b) Adiabatic change of the strength of coupling $J_n(t)$. (c) The trace distance defined in Eq. (42) for different target qubit state $\overline{\rho}_l$ at site $l = 3$. The solid, dashed, and dotted lines represent the results of target qubit states with different phase factors $\varphi = -0.82i$, 0, and $(\pi - 0.82i)$, respectively. (d) Purity of the reduced density matrix $\rho_l(t)$ for site $l = 3$ defined in Eq. (43)). Other parameters are $N = 5$, $\alpha = \beta = 1/\sqrt{2}$, and $\omega = 0.01$.

From Eq. (44) we have

$$\frac{1}{\sqrt{2}}\mathcal{U}(H^{\mathrm{L,R}})\big(\big|\psi_{\mathrm{e}}^{N}\big\rangle^{\mathrm{L,R}}\pm\big|\psi_{\mathrm{g}}^{N}\big\rangle^{\mathrm{L,R}}\big) = \frac{1}{\sqrt{2}}\big(|\uparrow\rangle_{l}^{\mathrm{L,R}}\pm e^{i\varphi}|\downarrow\rangle_{l}^{\mathrm{L,R}}\big)\prod_{j\neq l}^{N}|\downarrow\rangle_{j}^{\mathrm{L,R}}, \tag{45}$$

which results in

$$\frac{1}{\sqrt{2}}\mathcal{U}(H_{\mathrm{D}})\big(\big|\psi_{\mathrm{e}}^{N}\big\rangle^{\mathrm{L}}\big|\psi_{\mathrm{e}}^{N}\big\rangle^{\mathrm{R}}+\big|\psi_{\mathrm{g}}^{N}\big\rangle^{\mathrm{L}}\big|\psi_{\mathrm{g}}^{N}\big\rangle^{\mathrm{R}}\big) = \frac{1}{\sqrt{2}}\big(|\uparrow\rangle_{l}^{\mathrm{L}}|\uparrow\rangle_{l}^{\mathrm{R}}+e^{i2\varphi}|\downarrow\rangle_{l}^{\mathrm{L}}|\downarrow\rangle_{l}^{\mathrm{R}}\big)\prod_{j\neq l}^{N}|\downarrow\rangle_{j}^{\mathrm{L}}\prod_{j\neq l}^{N}|\downarrow\rangle_{j}^{\mathrm{R}}, \tag{46}$$

by direct derivation. Accordingly, it also provides a way to transfer the maximal pair entanglement from location i to l,

$$\frac{1}{\sqrt{2}}\big(|\uparrow\rangle_{i}^{\mathrm{L}}|\uparrow\rangle_{i}^{\mathrm{R}}+|\downarrow\rangle_{i}^{\mathrm{L}}|\downarrow\rangle_{i}^{\mathrm{R}}\big) \longrightarrow \frac{1}{\sqrt{2}}\big(|\uparrow\rangle_{l}^{\mathrm{L}}|\uparrow\rangle_{l}^{\mathrm{R}}+e^{i\varphi'}|\downarrow\rangle_{l}^{\mathrm{L}}|\downarrow\rangle_{l}^{\mathrm{R}}\big). \tag{47}$$

VI. DISCUSSION

In this paper, we have studied the relation between the gapped quasidegenerate ground states of an N-site Ising chain and that of the $(N+1)$-site chain, based on which the real-space renormalization method is developed. It allows us to build the effective Hamiltonian, which is an exactly solvable modified two-site Ising model and captures the low-energy physics of a given system. Numerical calculation shows that such an effective Hamiltonian has higher efficiency and is a feasible method for a large-size system. Due to the protection of the energy gap, this approximate description provides an alternative way to prepare the ground state and the first-excited state of an Ising chain on demand by dynamic processes of crystallization, generating robust macroscopic quantum states against disordered perturbation. To demonstrate the potential application of our finding, we proposed a scheme of entanglement transfer between a pair of qubits and two Ising chains, as macroscopic topological qubits. Our work, including the numerical result for a small size system, reveals that transverse field Ising chains can be utilized for developing inherently robust artificial devices for topological quantum information processing and communication.

ACKNOWLEDGMENTS

This work was supported by the National Natural Science Foundation of China (under Grant No. 11874225).

APPENDIX

In this Appendix, we will show the method of obtaining the nonlocal operator D_N in Eq. (4), as well as demonstrate its robustness. This method can also be used to analyze a non-Hermitian model [38]. Starting from the Ising chain H in Eq. (1) with uniform parameters $J_j = J$ and $g_j = g$, we first perform the Jordan-Wigner transformation [39]

$$\sigma_j^x = \prod_{l<j}(1-2c_l^\dagger c_l)(c_j+c_j^\dagger),$$
$$\sigma_j^y = i\prod_{l<j}(1-2c_l^\dagger c_l)(c_j-c_j^\dagger),$$
$$\sigma_j^z = 2c_j^\dagger c_j - 1 \tag{A1}$$

to replace the Pauli operators by the fermionic operators c_j. The Hamiltonian is transformed to a well-known Kitaev model

$$H_{\mathrm{Kitaev}} = J\sum_{j=1}^{N-1}(c_j^\dagger c_{j+1}+c_j^\dagger c_{j+1}^\dagger)+\mathrm{H.c.} + g\sum_{j=1}^{N}(2c_j^\dagger c_j-1). \tag{A2}$$

To get the solution of the model, we then introduce the Majorana fermion operators

$$a_j = c_j^\dagger + c_j,\quad b_j = -i(c_j^\dagger - c_j), \tag{A3}$$

which satisfy the commutation relations

$$\{a_j, a_{j'}\} = 2\delta_{j,j'},\quad \{b_j, b_{j'}\} = 2\delta_{j,j'},$$
$$\{a_j, b_{j'}\} = 0. \tag{A4}$$

Then the Majorana representation of the original Hamiltonian is

$$H_{\mathrm{M}} = \frac{i}{2}J\sum_{j=1}^{N-1}b_j a_{j+1} - \frac{i}{2}g\sum_{j=1}^{N}a_j b_j + \mathrm{H.c.}, \tag{A5}$$

the core matrix of which is that of a $2N$-site SSH chain in a single-particle invariant subspace. Based on the exact diagonalization result of the SSH chain, the Hamiltonian H_{Kitaev} can be written as the diagonal form

$$H_{\mathrm{Kitaev}} = \sum_{n=1}^{N}\varepsilon_n\left(d_n^\dagger d_n - \frac{1}{2}\right). \tag{A6}$$

Here d_n is a fermionic operator, satisfying $\{d_n, d_{n'}\} = 0$ and $\{d_n, d_{n'}^\dagger\} = \delta_{n,n'}$. On the other hand, we have the relations

$$[d_n, H_{\mathrm{Kitaev}}] = \varepsilon_n d_n,\quad [d_n^\dagger, H_{\mathrm{Kitaev}}] = -\varepsilon_n d_n^\dagger, \tag{A7}$$

which result in the mapping between the eigenstates of H_{Kitaev}. Direct derivation shows that, for an arbitrary eigenstate $|\psi\rangle$ of H_{Kitaev} with eigenenergy E, i.e.,

$$H_{\mathrm{Kitaev}}|\psi\rangle = E|\psi\rangle, \tag{A8}$$

state $d_n|\psi\rangle$ ($d_n^\dagger|\psi\rangle$) is also an eigenstate of H_{Kitaev} with the eigenenergy $E-\varepsilon_n$ ($E+\varepsilon_n$), i.e.,

$$H_{\mathrm{Kitaev}}(d_n|\psi\rangle) = (E-\varepsilon_n)(d_n|\psi\rangle) \tag{A9}$$

and

$$H_{\mathrm{Kitaev}}\big(d_n^\dagger|\psi\rangle\big) = (E+\varepsilon_n)\big(d_n^\dagger|\psi\rangle\big), \tag{A10}$$

if $d_n|\psi\rangle \neq 0$ ($d_n^\dagger|\psi\rangle \neq 0$).

Within the topological nontrivial region $|g/J| < 1$ ($g \neq 0$), the edge modes d_N and $d_N^\dagger$ appear with energy $\varepsilon_N = \pm|g/J|^N$.

This is responsible for the fact that the ground state and the first-excited state of the Ising chain in ordered phase are quasidegenerate in finite N (there is no edge mode in the trivial region $|g/J| \geqslant 1$). The edge operator d_N can be expressed as

$$d_N = \frac{1}{2}\sqrt{1-\left(\frac{g}{J}\right)^2}\sum_{j=1}^{N}\left\{\left[\left(-\frac{g}{J}\right)^{j-1}+\left(-\frac{g}{J}\right)^{N-j}\right]c_j^{\dagger} + \left[\left(-\frac{g}{J}\right)^{j-1}-\left(-\frac{g}{J}\right)^{N-j}\right]c_j\right\}, \tag{A11}$$

i.e., d_N is a linear combination of particle and hole operators of spinless fermions c_j on the edge, and we have $[d_N, H_{\text{Kitaev}}] = \varepsilon_N d_N = 0$ in the large N limit. Furthermore, applying the inverse Jordan-Wigner transformation, d_N can be expressed as the combination of spin operators,

$$D_N = \frac{1}{2}\sqrt{1-\left(\frac{g}{J}\right)^2}\sum_{j=1}^{N}\prod_{l<j}\left(-\sigma_l^z\right) \times\left[\left(-\frac{g}{J}\right)^{j-1}\sigma_j^x - i\left(-\frac{g}{J}\right)^{N-j}\sigma_j^y\right], \tag{A12}$$

In fact, d_N and D_N are identical, but only in different representations. Thus, from $[d_N, H_{\text{Kitaev}}] = 0$, we have

$$[D_N, H] = [D_N^{\dagger}, H] = 0, \tag{A13}$$

which leads to the degeneracy of the eigenstates. Furthermore, from the canonical commutation relations $\{d_N, d_N^{\dagger}\} = 1$ and $\{d_N, d_N\} = 0$, we have

$$\{D_N, D_N^{\dagger}\} = 1, \quad (D_N)^2 = (D_N^{\dagger})^2 = 0. \tag{A14}$$

For the Ising chain with slight disordered deviations on the uniform J and g, the operator D_N still exists and can be obtained by solving the Schrödinger equation for the corresponding SSH chain with random hopping in the single-particle invariant subspace [40]. We have the following solution:

$$D_N = \frac{1}{2}\sum_{j=1}^{N}\prod_{l<j}\left(-\sigma_l^z\right)\left(h_j^{+}\sigma_j^x - ih_j^{-}\sigma_j^y\right), \tag{A15}$$

where

$$h_j^{+} = h_1^{+}\prod_{m=1}^{j-1}\left(-\frac{g_m}{J_m}\right),$$
$$h_j^{-} = h_N^{-}\left(-\frac{g_N}{J_j}\right)\prod_{m=j+1}^{N-1}\left(-\frac{g_m}{J_m}\right), \tag{A16}$$

and h_1^{+} (h_N^{-}) is determined by the normalization condition $\sum_{j=1}^{N}|h_j^{\pm}|^2 = 1$. The solution of D_N is robust against disordered perturbation and the corresponding energies of the edge modes are still exponentially small in N under the condition that the average value of J_m is stronger than the average value of g_m [40]. Then it can be checked that the commutation relations in Eqs. (A13) and (A14) still hold for the operator D_N with disordered perturbation in the large-N limit.

[1] P. Pfeuty, The one-dimensional Ising model with a transverse field, Ann. Phys. (NY) **57**, 79 (1970).

[2] S. Sachdev, *Quantum Phase Transitions* (Cambridge University Press, Cambridge, England, 1999).

[3] G. Zhang and Z. Song, Topological Characterization of Extended Quantum Ising Models, Phys. Rev. Lett. **115**, 177204 (2015).

[4] G. Zhang, C. Li, and Z. Song, Majorana charges, winding numbers and Chern numbers in quantum Ising models, Sci. Rep. **7**, 8176 (2017).

[5] A. Y. Kitaev, Unpaired Majorana fermions in quantum wires, Phys. Usp. **44**, 131 (2001).

[6] R. Botet, R. Jullien, and M. Kolb, Finite-size-scaling study of the spin-1 Heisenberg-Ising chain with uniaxial anisotropy, Phys. Rev. B **28**, 3914 (1983).

[7] M. P. Nightingale and H. W. J. Blöte, Gap of the linear spin-1 Heisenberg antiferromagnet: A Monte Carlo calculation, Phys. Rev. B **33**, 659(R) (1986).

[8] S. R. White and D. A. Huse, Numerical renormalization-group study of low-lying eigenstates of the antiferromagnetic $S = 1$ Heisenberg chain, Phys. Rev. B **48**, 3844 (1993).

[9] S. R. White and I. Affleck, Spectral function for the $S = 1$ Heisenberg antiferromagetic chain, Phys. Rev. B **77**, 134437 (2008).

[10] Y. P. Shim, A. Sharma, C. Y. Hsieh, and P. Hawrylak, Artificial Haldane gap material on a semiconductor chip, Solid State Commun. **150**, 2065 (2010).

[11] W. J. L. Buyers, R. M. Morra, R. L. Armstrong, M. J. Hogan, P. Gerlach, and K. Hirakawa, Experimental Evidence for the Haldane Gap in a Spin-1 Nearly Isotropic, Antiferromagnetic Chain, Phys. Rev. Lett. **56**, 371 (1986).

[12] R. M. Morra, W. J. L. Buyers, R. L. Armstrong, and K. Hirakawa, Spin dynamics and the Haldane gap in the spin-1 quasi-one-dimensional antiferromagnet $CsNiCl_3$, Phys. Rev. B **38**, 543 (1988).

[13] E. Čižmár, M. Ozerov, O. Ignatchik, T. P. Papageorgiou, J. Wosnitza, S. A. Zvyagin, J. Krzystek, Z. Zhou, C. P. Landee, B. R. Landry, M. M. Turnbull, and J. L. Wikaira, Magnetic properties of the Haldane-gap material $[Ni(C_2H_8N_2)_2NO_2](BF_4)$, New J. Phys. **10**, 033008 (2008).

[14] F. Delgado, C. D. Batista, and J. Fernández-Rossier, Local Probe of Fractional Edge States of $S = 1$ Heisenberg Spin Chains, Phys. Rev. Lett. **111**, 167201 (2013).

[15] C. Rüegg, N. Cavadini, A. Furrer, H.-U. Güdel, K. Krämer, H. Mutka, A. Wildes, K. Habicht, and P. Vorderwisch, Bose-Einstein condensation of the triplet states in the magnetic insulator $TlCuCl_3$, Nature (London) **423**, 62 (2003).

[16] H. M. Rønnow, R. Parthasarathy, J. Jensen, G. Aeppli, T. F. Rosenbaum, and D. F. McMorrow, Quantum phase transition of a magnet in a spin bath, Science **308**, 389 (2005).

[17] J. Simon, W. S. Bakr, R. Ma, M. E. Tai, P. M. Preiss, and M. Greiner, Quantum simulation of antiferromagnetic spin chains in an optical lattice, Nature (London) **472**, 307 (2010).

[18] F. D. M. Haldane, Nonlinear Field Theory of Large-Spin Heisenberg Antiferromagnets: Semiclassically Quantized Solitons of the One-Dimensional Easy-Axis Néel State, Phys. Rev. Lett. **50**, 1153 (1983).

[19] I. Affleck, T. Kennedy, E. H. Lieb, and H. Tasaki, Valence bond ground states in isotropic quantum antiferromagnets, Commun. Math. Phys. **115**, 477 (1988).

[20] I. Affleck, Quantum spin chains and the Haldane gap, J. Phys.: Condens. Matter **1**, 3047 (1989).

[21] M. Hagiwara, K. Katsumata, I. Affleck, B. I. Halperin, and J. P. Renard, Observation of $S = 1/2$ degrees of Freedom in an $S = 1$ Linear-Chain Heisenberg Antiferromagnet, Phys. Rev. Lett. **65**, 3181 (1990).

[22] S. H. Glarum, S. Geschwind, K. M. Lee, M. L. Kaplan, and J. Michel, Observation of Fractional Spin $S = 1/2$ on Open Ends of $S = 1$ Linear Antiferromagnetic Chains: Nonmagnetic Doping, Phys. Rev. Lett. **67**, 1614 (1991).

[23] J. Xu, Q. Gu, and E. J. Mueller, Realizing the Haldane Phase with Bosons in Optical Lattices, Phys. Rev. Lett. **120**, 085301 (2018).

[24] J. R. Petta, A. C. Johnson, J. M. Taylor, E. A. Laird, A. Yacoby, M. D. Lukin, C. M. Marcus, M. P. Hanson, and A. C. Gossard, Coherent manipulation of coupled electron spins in semiconductor quantum dots, Science **309**, 2180 (2005).

[25] M. Korkusinski, and P. Hawrylak, Coded qubits based on electron spin, in *Semiconductor Quantum Bits*, edited by O. Benson and F. Henneberger (World Scientific, Singapore, 2008), pp. 3–32.

[26] M. W. Johnson, M. H. S. Amin, S. Gildert, T. Lanting, F. Hamze, N. Dickson, R. Harris, A. J. Berkley, J. Johansson, P. Bunyk, E. M. Chapple, C. Enderud, J. P. Hilton, K. Karimi, E. Ladizinsky, N. Ladizinsky, T. Oh, I. Perminov, C. Rich, M. C. Thom, E. Tolkacheva, C. J. S. Truncik, S. Uchaikin, J. Wang, B. Wilson, and G. Rose, Quantum annealing with manufactured spins, Nature (London) **473**, 194 (2011).

[27] C.-Y. Hsieh, Y. P. Shim, M. Korkusinski, and P. Hawrylak, Physics of lateral triple quantum-dot molecules with controlled electron numbers, Rep. Prog. Phys. **75**, 114501 (2012).

[28] S. D. Sarma, M. Freedman, and C. Nayak, Majorana zero modes and topological quantum computation, npj Quantum Inf. **1**, 15001 (2015).

[29] C. Nayak, S. H. Simon, A. Stern, M. Freedman, and S. D. Sarma, Non-Abelian anyons and topological quantum computation, Rev. Mod. Phys. **80**, 1083 (2008).

[30] A. Stern, Non-Abelian states of matter, Nature (London) **464**, 187 (2010).

[31] J. Alicea, New directions in the pursuit of Majorana fermions in solid state systems, Rep. Prog. Phys. **75**, 076501 (2012).

[32] W. P. Su, J. R. Schrieffer, and A. J. Heeger, Solitons in Polyacetylene, Phys. Rev. Lett. **42**, 1698 (1979).

[33] P. Fendley, Strong Zero Modes and Eigenstate Phase Transitions in the XYZ/Interacting Majorana Chain, J. Phys. A **49**, 30LT01 (2016).

[34] S. Katsura, Statistical Mechanics of the Anisotropic Linear Heisenberg Model, Phys. Rev. **127**, 1508 (1962).

[35] A. Einstein, B. Podolsky, and N. Rosen, Can Quantum-Mechanical Description of Physical Reality Be Considered Complete? Phys. Rev. **47**, 777 (1935).

[36] J. S. Bell, *Speakable and Unspeakable in Quantum Mechanics* (Cambridge University Press, Cambridge, UK, 1988).

[37] R. Horodecki, P. Horodecki, M. Horodecki, and K. Horodecki, Quantum entanglement, Rev. Mod. Phys. **81**, 865 (2009).

[38] K. L. Zhang and Z. Song, Ising chain with topological degeneracy induced by dissipation, Phys. Rev. B **101**, 245152 (2020).

[39] P. Jordan and E. Wigner, Über das paulische ä quivalenzverbot, Z. Phys. **47**, 631 (1928).

[40] J. K. Asbóth, L. Oroszlány, and A. P ályi, *A Short Course on Topological Insulators: Band Structure and Edge States in One and Two Dimensions*, Lecture Notes in Physics (Springer International Publishing, Switzerland, 2016).